

Local moment fluctuations in an optimally-doped high T_c superconductor

D. Reznik,^{1,2} J.-P. Ismer,^{3,4} I. Eremin,^{3,4} L. Pintschovius,¹ T. Wolf,¹ M. Arai,⁵ Y. Endoh,⁶ T. Masui,⁷ and S. Tajima⁷

¹*Forschungszentrum Karlsruhe, Institut für Festkörperphysik, Postfach 3640, D-76021 Karlsruhe, Germany*

²*Laboratoire Leon Brillouin, C.E.A./C.N.R.S., F-91191-Gif-sur-Yvette CEDEX, France*

³*Max-Planck-Institut für Physik Komplexer Systeme, D-01187 Dresden, Germany*

⁴*Institute für Mathematische und Theoretische Physik,
TU-Braunschweig, 38106 Braunschweig, Germany*

⁵*Institute of Materials Structure Science, KEK, Tsukuba 305-0801, Japan*

⁶*Synchrotron Radiation Research Center, Japan Atomic Energy Research Institute, Hyogo 679-5148, Japan*

⁷*Department of Physics, Osaka University, Toyonaka, Osaka 560-0043, Japan*

(Dated: June 27, 2018)

We present results of neutron scattering experiments on $\text{YBa}_2\text{Cu}_3\text{O}_{6.95}$ ($T_c=93\text{K}$). Our results indicate that magnetic collective modes due to correlated local moments are present both above and below T_c in optimally doped YBCO. The magnon-like modes are robust and not overdamped by itinerant particle-hole excitations, which may point at a substantial static or slowly fluctuating charge inhomogeneity. We compare the experimental results to predictions of the Fermi liquid (FL) theory in the Random Phase Approximation (RPA).

PACS numbers: 74.72.-h, 74.25.Gz, 74.20.Mn

High temperature superconductivity occurs in layered copper oxides at compositions between undoped insulating and strongly doped conventional metallic phases. Some propose that exotic states inherited from the antiferromagnetic parent Mott insulators are essential for superconductivity¹ whereas others claim that superconductors with the highest transition temperatures, T_c , conform to the standard model of metals, the Fermi liquid theory².

Magnetic spectra of the copper oxides change dramatically as a function of doping. At $x = 0$, these compounds are Mott insulators with strong on-site repulsion that localizes electrons whose spins order antiferromagnetically. Their low energy excitations are spin waves (magnons), which disperse upward from the antiferromagnetic (AF) ordering vector^{4?}. Doping disrupts long range AF order, but dispersive excitations similar to magnons remain in underdoped superconductors ($0 < x < .13$) at high energies^{5,6,7,8}. However, such magnetic excitations have not so far been detected in superconductors with $T_c > 80\text{K}$. Previous experimental studies of the compounds with the highest T_c s focused primarily on the resonance feature around $40\text{meV}^{9,10,11}$ appearing only below T_c^{12} . Both Fermi liquid and non-Fermi liquid scenarios have been proposed to explain the resonance^{1,2,5,13,14,15,16,17}.

Here, we focus on magnetic excitations in optimally doped $\text{YBa}_2\text{Cu}_3\text{O}_{6.95}$ ($T_c = 93\text{ K}$) above T_c . Since previous studies failed to clearly distinguish^{12,18} the magnetic signal from the nuclear background, we used much longer counting times (more than 1hr/point in some scans) to significantly reduce statistical error. We report that the collective magnetic excitations do exist in $\text{YBa}_2\text{Cu}_3\text{O}_{6.95}$ and that their intensity is appreciable in comparison to the magnon intensity in the parent insulator and the underdoped $\text{YBa}_2\text{Cu}_3\text{O}_{6.6}$.

The experiments were performed on the 1T triple-axis

spectrometer at the ORPHEE reactor at Saclay utilizing a double focusing Cu111 monochromator and a pyrolytic graphite (PG002) analyzer. The high quality sample of $\text{YBa}_2\text{Cu}_3\text{O}_{6.95}$ was the same as in an earlier study¹⁹.

Following Ref. 20, magnetic collective modes were separated from the nuclear background by subtracting spectra recorded at a high temperature where the magnetic modes are largely suppressed. Fig. 1(a) and (b) give examples of the raw data at 52.5 and 60 meV where there is a clear double peak structure around $h=0.5$, the AF wavevector of the undoped parent compounds, at 10K and 100K. The intensity of this feature is reduced on heating above 300K, as expected from magnetic collective modes. Some or all intensity that remains at the high temperatures may be magnetic but to be on the conservative side, we subtract the entire high T spectrum divided by the Bose factor from the 10K and 100K data.

The measured energies were chosen to minimize systematic errors due to contamination by nuclear scattering. The biggest error in our experiment is an underestimate of the magnetic signal because some of it (10-20%) may remain at high temperatures where the background was measured. Any broad continuum is indistinguishable from the background and is also not included in the extracted intensities. Fig. 2 shows that normal state magnetic intensity extracted by this procedure obeys crystal symmetry appearing with a similar intensity in the vicinity of equivalent AF wavevectors $\mathbf{Q} = (1.5, 0.5, 1.7)$ and $(1.5, -0.5, 1.7)$. The observed magnetic signal was centered at equivalent antiferromagnetic wavevectors $\mathbf{Q} = (1.5, 0.5, 1.7)$, $\mathbf{Q} = (0.5, 0.5, 5.4)$, and $\mathbf{Q} = (1.5, 1.5, 1.7)$ in units of $(2\pi/a, 2\pi/b, 2\pi/c)$, (where a , b , and c are lattice constants (data not shown for the latter)). Its intensities in different Brillouin zones agree with the magnetic form factor confirming the validity of this procedure. Since YBCO is a bi-layer compound, it has magnetic excitations of acoustic and optic

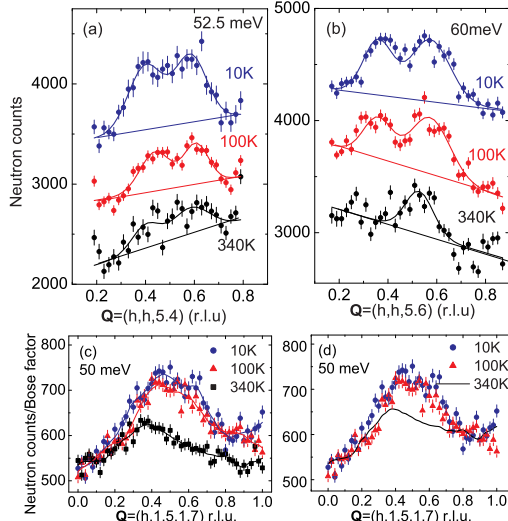


FIG. 1: (Color online) Raw data and background subtraction procedure. (a,b) Scans at 52.5 and 60meV at 10K, 100K, and 340K offset by a constant for clarity. Lines are guides to the eye. Note that the peak in (b) at 340K is most certainly nonmagnetic. (c) Scans at 50meV through the anti-ferromagnetic wave vector divided by the Bose factor. Solid lines represent smoothed data. The feature centered at $h=0.5$ at 10K and 100K is magnetic because it is suppressed at 330K as the underlying correlations become weaker, leaving behind a "hump" of nuclear scattering peaked at $h=0.4$. The background levels near $h=0$ and $h=1$ do not exactly match due to small nuclear contributions whose temperature-dependence does not follow the Bose factor (e.g. multi-phonon or incoherent elastic nuclear scattering). Linear corrections were added to the 100K and 330K data to match the backgrounds near $h=0$ and $h=1$ with the result shown in (b). These corrections were small in all cases (the 50 meV data are the worst case); (d) 50 meV scans after adding the linear terms to the 100K and 330K data. We assign the intensity difference between 10K/100K data and 330K curve to magnetic scattering. Error bars represent s.d.

character. Our choice of $L=1.7$ and 5.4 selects acoustic magnetic excitations; a separate study will be necessary to investigate optic modes.

Fig. 3 shows the magnon scattering intensity of insulating $\text{YBa}_2\text{Cu}_3\text{O}_{6.1}$ and of the underdoped $T_c=60\text{K}$ superconductor, $\text{YBa}_2\text{Cu}_3\text{O}_{6.6}$, at 52.5meV plotted together with that of the optimally-doped sample at 100K on the same intensity scale. IN the underdoped samples it was obtained by subtracting a constant background since significant magnetic intensity is still present at 300K. To correct for sample volume we scaled together spectra of the bond-buckling phonon at $E = 42.5$ meV. Its eigenvector is independent of doping because it does not contain any chain oxygen vibrations¹². The phonon was measured in identical spectrometer configurations (at $\mathbf{Q} = (0.5, 0.5, 11)$) in the two samples (Fig. 3a). Therefore, no resolution corrections were needed. The magnon peak intensity in $\text{YBa}_2\text{Cu}_3\text{O}_{6.1}$ is six times

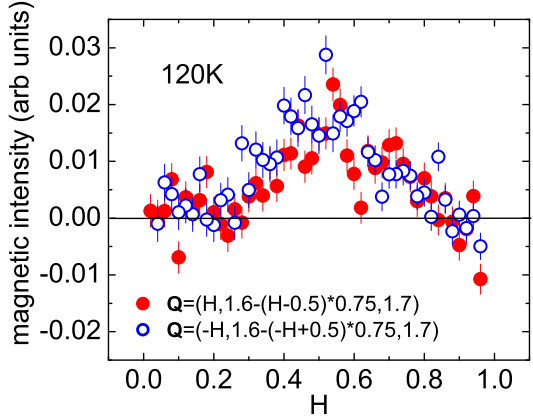


FIG. 2: (Color online) Magnetic intensity at 120K at 55meV extracted by the procedure described in the text and Fig. 1. The data in the vicinity of equivalent AF wave vectors $\mathbf{Q} = (1.5, 0.5, 1.7)$ (left panel) and $\mathbf{Q} = (1.5, -0.5, 1.7)$ (right panel) are shown in arbitrary units but on the same scale. Small differences between the two curves are consistent with different resolution functions at the two wavevectors and/or statistical error. This figure demonstrates that the intensity that we assign to magnetic scattering has the correct symmetry.

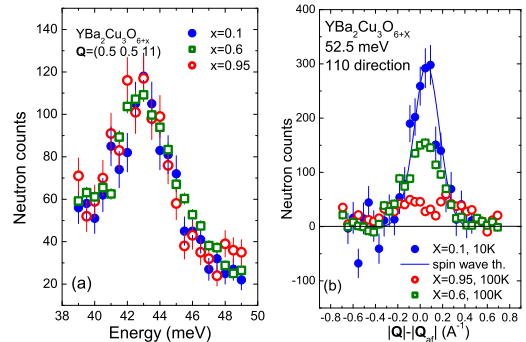


FIG. 3: (Color online) Comparison of magnetic scattering of the $\text{YBCO}_{6.1}$ $\text{YBCO}_{6.6}$, and $\text{YBCO}_{6.95}$ samples.(a) Spectra of the Cu-O buckling mode scaled by the factor equal to the ratio of the volumes of the three samples. (b) Magnetic scattering intensities plotted on the same intensity scale after normalization by the volume ratio extracted from comparison of phonon intensities in (a).

stronger than that of the normal state magnetic signal in $\text{YBa}_2\text{Cu}_3\text{O}_{6.95}$ whereas the peak intensity of the $T_c=60\text{K}$ sample measured at 100K was three times stronger. However, the magnetic signal in $\text{YBa}_2\text{Cu}_3\text{O}_{6.95}$ is significantly broader than in the insulating phase and in the underdoped sample (In the insulator it is nearly \mathbf{Q} -resolution-limited). Thus their \mathbf{q} -integrated intensities of the three samples must be of the same order of magnitude around 50meV at 100K after two-dimensional \mathbf{Q} -integration. In making this statement, we are assum-

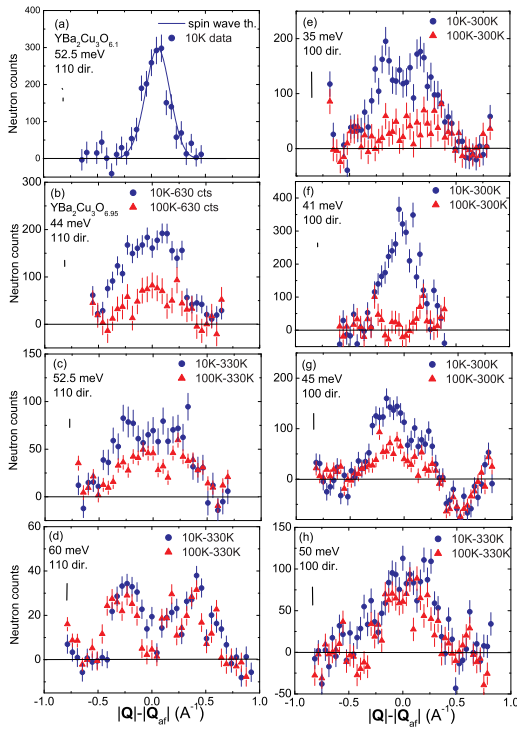


FIG. 4: (Color online) Magnetic intensities at different energies. (a) Magnon peak in $\text{YBa}_2\text{Cu}_3\text{O}_{6.1}$ at 52.5 meV after subtraction of a flat background. Solid line represents the spin wave model in Ref.⁶ convoluted with the spectrometer resolution. (b-h) Magnetic scattering in $\text{YBa}_2\text{Cu}_3\text{O}_{6.95}$ as a function of the distance from the antiferromagnetic ordering wave vector. All spectra have been normalized to the same scale. A constant background of 530 and 630 counts was subtracted in (a) and (b) respectively, whereas the other magnetic spectra were obtained as described in the text and Fig.1. The weak broad 100K signal at 35meV may be an artifact of the background subtraction procedure. Error bars represent s.d. Our estimate of systematic errors given by vertical black lines is based on the temperature variation of the background.

ing that magnetic scattering is broad in \mathbf{q} and has a fourfold symmetry around the reduced antiferromagnetic wave vector $\mathbf{Q}_{AF}=(0.5,0.5)$ in a twinned sample like ours.

Fig. 4 (b-h) shows magnetic spectra of $\text{YBa}_2\text{Cu}_3\text{O}_{6.95}$ measured at different energies at 10K and 100K, respectively, and Fig. 5(a,b) shows the cut along [110] after removing effects of the resolution. It is based on the data shown in Fig. 4 and Ref. 19. At 100K we observe a branch above 43 meV dispersing away from \mathbf{Q}_{AF} . Its \mathbf{q} -width is 0.3\AA^{-1} full width at half maximum (FWHM), which corresponds to a correlation length of about 20\AA . Upon cooling to 10K, the scattering intensity below 60 meV increases and a downward-dispersing branch with a constant \mathbf{q} -integrated intensity appears between 33 and 41 meV below T_c as shown in Refs. 19,20. The \mathbf{q} -width of the lower branch is relatively narrow (Fig. 5(a)), corresponding to coherent domains of about 55\AA^{19} . The upward-dispersing branch is signifi-

cantly less steep than the magnon dispersion in insulating $\text{YBa}_2\text{Cu}_3\text{O}_{6.1}$. (Fig. 5a,b) Assuming linear extrapolation, it crosses the zone boundary around 130/100 meV in the [100]/[110] direction, respectively, compared with 220meV for the magnons in the insulator⁴. It also disperses significantly less steeply than the upper branch in $\text{YBa}_2\text{Cu}_3\text{O}_{6.6}$, which has a much narrower lineshape at 52.5meV (Fig. 3) with the magnetic intensity remaining near to $\mathbf{q}=(0.5,0.5)$.⁷

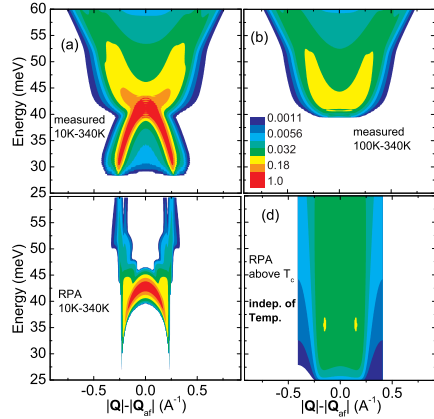


FIG. 5: (Color online) Magnetic susceptibility of $\text{YBa}_2\text{Cu}_3\text{O}_{6.95}$. (a/b) Experimentally measured magnetic susceptibility difference between 10K/100K respectively and 300K in the 110 direction after removing effects of the resolution. Different ad. hoc. functional forms were tried until their convolution with the spectrometer resolution agreed with the data. (c) Calculations based on FL/RPA (Ref.¹⁵) for the difference between the superconducting state (10K) and normal state (300K). (d) RPA result for the normal state. Here the difference between 100K and 300K is negligibly small (in contrast with experiment), so only 100K result is shown without taking the difference. Note the logarithmic intensity scale when comparing experimental and calculated spectra.

Fig. 5(c,d) shows the prediction of the FL theory in the standard RPA approximation (FL/RPA)^{13,14,15,16} using the calculation based on Ref.¹⁶. The RPA expression for the spin susceptibility is:

$$\chi_{RPA}^{+-}(\mathbf{q}, \omega) = \frac{\chi_0^{+-}(\mathbf{q}, \omega)}{1 - g_{\mathbf{q}}\chi_0^{+-}(\mathbf{q}, \omega)} \quad (1)$$

where $\chi_0^{+-}(\mathbf{q}, \omega)$ is the bare transverse susceptibility and $g_{\mathbf{q}}$ is an electron-electron interaction (four-point vertex), which in general can be momentum dependent^{13,14,15,16}. Once the parameters of the model were picked to reproduce the known Fermi surface, band width of optimally-doped copper oxides, the superconducting gap²¹, and the resonance peak energy, there was no further possibility to adjust parameters to alter the calculation results in any significant way. Imaginary part of $\chi_{RPA}^{+-}(\mathbf{q}, \omega)$ is proportional to the neutron scattering cross section and can be directly compared with experiment. Below T_c sharp

downward-dispersing resonance collective modes appear in the calculation due to an excitonic effect inside the $d_{x^2-y^2}$ -wave superconducting gap (Fig. 5c)¹⁶. This feature appears to be in good agreement with the experiment (Fig. 5 a,c). The calculation also predicts an upward-dispersing feature below T_c . However it is an order of magnitude weaker (relative to the downward-dispersing branch) and has a steeper effective dispersion than the measured magnetic signal.

Above T_c FL/RPA predicts only a broad temperature-independent particle-hole continuum and no collective modes (Fig. 5d). Within a simple Fermi-liquid picture one expects weak temperature dependence of the $\text{Im}\chi$ proportional to the $k_B T/E_F$ with E_F being the Fermi energy. In optimally-doped YBCO this ratio is too small to be detected at the energies that we probed. In contrast with the FL/RPA result, our experiment shows that the spin signal grows significantly on cooling from 340K to 100K. Including the renormalization of the quasiparticles due to scattering by the spin fluctuations within a so-called fluctuation exchange approximation (FLEX) yields a much stronger temperature dependence of the spin excitations at low energies but not at the high energies that we investigated²². It is not entirely clear how further renormalization of the interaction strength (vertex corrections) will affect the results of the FLEX calculation. Our preliminary estimate is that it will further reduce the predicted temperature dependence.

The above analysis leads us to conclude that the FL/RPA picture does explain magnetic intensity above $\sim 45\text{meV}$ in neither the normal state nor in the superconducting state. The 52.5 and 60 meV data (Figs. 1, 3c,d) show incommensurate collective modes both above and below T_c whose dispersion is similar to magnons in the parent insulator. (Fig. 5b) (Note that the scans at 55meV in Fig. 2 do not have a double-peak structure be-

cause they were centered not at $Q=(1.5 0.5 1.7)$, but at one of the incommensurate satellites: $Q=(1.6 0.5 1.7)$.) Based on this observation we assign these modes to collective excitations of local moments inherited from the insulating phase^{23,24,25,26} as opposed to itinerant quasiparticles inherited from the overdoped conventional FL phase. These local moments must coexist with the itinerant particle-hole continuum spanned by the Fermi surface.

Our results suggest a qualitative similarity between the YBCO family and the $\text{La}_{2-x}\text{Sr}_x\text{CuO}_4$ family of high T_c superconductors. Wakimoto et al.²⁷ found that low energy magnetic excitations peaked near \mathbf{Q}_{AF} disappear upon increased doping whereas the high energy fluctuations persist far into the overdoped regime²⁸. In $\text{YBa}_2\text{Cu}_3\text{O}_{6+x}$ the lowest energy for detecting magnetic excitations due to local moments also increases with increasing doping reaching approximately 45 meV at optimal doping as shown in our investigation. This apparent gap in the measurable magnetic signal probably appears because the magnetic modes are not magnons in the strict sense but rather precursor fluctuations to the formation of antiferromagnetic clusters. Developing a detailed theory of this phenomenon is outside the scope of our study.

One possibility that can be ruled out is that our sample may still be in the pseudogap state at 100K and thus the observed local magnetism is associated with the pseudogap. Figure 2 shows that the magnetic signal persist at least up to 120K, which is above the pseudogap temperature reported for $T_c=93\text{K}$ YBCO. Thus the magnetic signal above T_c at optimal doping is not associated with the pseudogap.²⁹

Acknowledgement: D.R. would like to thank S.A. Kivelson, J. Zaanen, and M. Vojta for valuable comments on earlier versions of the manuscript. I.E. would like to thank T. Dahm for helpful discussions.

¹ P.A. Lee, N. Nagaosa, and X.-G. Wen, Rev. Mod. Phys. **78**, 17 (2006).

² Ar. Abanov, A.V. Chubukov, and J. Schmalian, Adv. Phys. **52**, 119 (2003).

³ J.M. Tranquada, G. Shirane, B. Keimer, S. Shamoto, and M. Sato, Phys. Rev. B **40** 4503 (1989).

⁴ S.M. Hayden, G. Aeppli, T.G. Perring, H.A. Mook, and F. Dogan, Phys. Rev. B **54**, R6905 (1996).

⁵ M. Arai, T. Nishijima, Y. Endoh, T. Egami, S. Tajima, K. Tomimoto, Y. Shiohara, M. Takahashi, A. Garrett, and S. M. Bennington, Phys. Rev. Lett. **83**, 608 (1999).

⁶ J. M. Tranquada, H. Woo, T. G. Perring, H. Goka, G. D. Gu, G. Xu, M. Fujita, and K. Yamada, Nature **429**, 534 (2004).

⁷ S. Hayden, H.A. Mook, Pengcheng Dai, T.G. Perring, and F. Dogan, Nature **429**, 531 (2004).

⁸ V. Hinkov, P. Bourges, S. Pailhes, Y. Sidis, A. Ivanov, C. D. Frost, T. G. Perring, C. T. Lin, D. P. Chen, and B. Keimer, Nature Physics **3**, 780 (2007).

⁹ J. Rossat-Mignod, L. P. Regnault, C. Vettier, P. Bourges, P. Burlet, J. Bossy, J. Y. Henry, and G. Lapertot, Physica C **185-189**, 86 (1991).

¹⁰ H. He, P. Bourges, Y. Sidis, C. Ulrich, L. P. Regnault, S. Pailhs, N. S. Berzigarova, N. N. Kolesnikov, and B. Keimer, Science **295**, 1045 (2002).

¹¹ H. F. Fong, P. Bourges, Y. Sidis, L. P. Regnault, A. Ivanov, G. D. Gu, N. Koshizuka, and B. Keimer, Nature **398**, 588 (1999);

¹² H.F. Fong, B. Keimer, P.W. Anderson, D. Reznik, F. Dogan, and I.A. Aksay, Phys. Rev. Lett. **75**, 316 (1995).

¹³ E. Demler, and S.C. Zhang, Phys. Rev. Lett. **75**, 4126 (1995).

¹⁴ D.Z. Liu, Y. Zha, and K. Levin, Phys. Rev. Lett. **75**, 4130 (1995).

¹⁵ F. Onufrieva, and P. Pfeuty, Phys. Rev. B **65**, 054515 (2002).

¹⁶ I. Eremin, D.K. Morr, A.V. Chubukov, K.-H. Bennemann, and M.R. Norman, Phys. Rev. Lett. **94**, 147001 (2005).

¹⁷ M. Vojta, T. Vojta, and R.K. Kaul, Phys. Rev. Lett. **97**, 097001 (2006).

¹⁸ Hyungje Woo, Pengcheng Dai, S. M. Hayden, H. A. Mook, T. Dahm, D. J. Scalapino, T. G. Perring, and F. Dogan, Nat. Physics **2**, 604 (2006).

¹⁹ D. Reznik, P. Bourges, L. Pintschovius, Y. Endoh, Y. Sidis, T. Masui, and S. Tajima, Phys. Rev. Lett. **93**, 207003 (2004).

²⁰ P. Bourges, Y. Sidis, H. F. Fong, L. P. Regnault, J. Bossy, A. Ivanov, B. Keimer, Science **288**, 1234 (2000).

²¹ A. Damascelli, Z. Hussain, and Z.-X. Shen, Rev. Mod. Phys. **75**, 473 (2003).

²² T. Dahm and L. Tewordt, Phys. Rev. B **52**, 1297 (1995).

²³ C.D. Batista, G. Ortiz, and A.V. Balatsky, Phys. Rev. B **64**, 172508 (2001).

²⁴ M.V. Eremin, A.A. Aleev, and I.M. Eremin, Zhur. Eksp. Teor. Fiz. **133**, 862 (2008). [JETP **106**, 752 (2008)].

²⁵ I. Sega, P. Prelovsek, and J. Bonca, Phys. Rev. B **68**, 054524 (2003).

²⁶ A. Sherman and M. Schreiber, Phys. Rev. B **68**, 094519 (2003).

²⁷ S. Wakimoto, K. Yamada, J. M. Tranquada, C. D. Frost, R. J. Birgeneau, and H. Zhang, Phys. Rev. Lett. **98**, 247003 (2007).

²⁸ O.J. Lipscombe, S.M. Hayden, B. Vignolle, D.F. McMorrow, and T.G. Perring, Phys. Rev. Lett. **99**, 067002 (2007).

²⁹ S.H. Naqib, J.R. Cooper, J.L. Tallon, R.S. Islam, and R.A. Chakalov, Phys. Rev. B **71**, 054502 (2005).